24X-H2C6E2D2B2

Fundamentals, Computer Implementation and Applications of the Advanced Compact MOSFET (ACM) Model

O. Franca Siebel, M. C. Schneider, and C. Galup-Montoro

Department of Electrical Engineering, Federal University of Santa Catarina, Florianópolis, SC, CEP 88040-900, Brazil.

In this study we introduce a new computer implementation of the advanced compact MOSFET (ACM) model. The core ACM model, its computer implementation and some simulation tests are presented.

Introduction

Based essentially on the gradual channel approximation, the Pao-Sah formula has served as a reference to test the accuracy of compact models (1), but has been considered numerically too involved to be used as the core of a compact model. With the addition of the charge sheet approximation to the gradual channel approximation, surface potential models have been developed since the pioneering work in (2). The main drawbacks of these first generation surface potential models are their cumbersome expressions for total charges and capacitances. To simplify the current and total stored charge expressions, the linearization of the depletion charge terms has been widely adopted (3)-(5).

In this study after reviewing the Pao-Sah formula and the main approximations for compact models, we discuss the consistency of the compact equation for the current with the Pao-Sah formulation. A very simple fully-consistent model is obtained, which is reviewed in the fourth Section. Its computer implementation is summarized in the fifth Section and some simulation benchmarks and comparisons with other models are presented in the sixth Section.

Pao-Sah Current Expression

The Pao-Sah current equation (6) is

$$I_D = -\mu W Q'_I \frac{dV_C}{dy} \qquad [1]$$

where W is the channel width, μ is the carrier mobility, Q'_I is the inversion charge density, y the distance along the channel, and V_C is the channel potential, varying between V_S and V_D, the source-to-bulk and drain-to-bulk potentials, respectively. Expression [1] includes both the drift and diffusion transport mechanisms, and gives an exact model of the long-channel MOSFET. For this reason Eq. [1] is used as a golden reference to test the accuracy of compact models.

Since the current is constant along the channel, the integration of Eq. [1] from source to drain, yields

$$I_D = -\frac{W}{L}\int_{V_S}^{V_D} \mu Q'_I(V_C)\,dV_C \qquad [2]$$

where L is the channel length.

The small-signal output conductance of the transistor is defined as

$$g_d = \left.\frac{\partial I_D}{\partial V_D}\right|_{V_G, V_S} \qquad [3]$$

where V_G *is* the gate-to-bulk potential.

Applying the definition of Eq. [3] to the Pao-Sah formula [1], we obtain

$$g_d = -\mu \frac{W}{L} Q_I'(V_D)\,. \qquad [4]$$

It is remarkable that the very simple Eq. [4] is valid from weak inversion (where the current transport is dominated by diffusion) to strong inversion (where drift dominates).

Basic Approximations for Compact Models

Charge-sheet Approximation

Representing the three-terminal MOS structure by a capacitive model (7) as shown in Figure 1, it follows that

$$dQ_I' = C_i'\left(dV_C - d\phi_s\right) \qquad [5]$$

where C'_i is the inversion capacitance and ϕ_s is the surface potential.

The charge-sheet approximation assumes that the inversion layer has zero thickness. It can be shown that the inversion capacitance reduces using this approximation to

$$C_i' = -\frac{Q_I'}{\phi_t}\,. \qquad [6]$$

It is worth observing that [6] is only exact in weak inversion. In effect, the resolution of the Poisson equation in the semiconductor shows that the logarithmic slope of the Q'_I (ϕ_s) curve varies from $1/\phi_t$ in weak inversion to $1/2\phi_t$ deep in strong inversion (8).

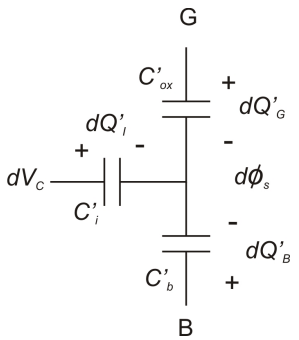

Figure 1. Small-signal model for the three terminal MOSFET.

Substituting [6] into [5] we get (9)

$$\frac{dV_C}{d\phi_s} = 1 - \frac{\phi_t}{Q_I'}\frac{dQ_I'}{d\phi_s}. \qquad [7]$$

Finally, from [1] and [7] the charge sheet current expression results.

$$I_D = I_{drift} + I_{diff} = -\mu W Q_I' \frac{d\phi_s}{dy} + \mu W \phi_t \frac{dQ_I'}{dy} \qquad [8]$$

where the first term correspond to the drift and the second to the diffusion component of the current.

Linearization of the inversion charge density vs. surface potential relationship

In the charge sheet approximation, the inversion charge density is calculated as the total semiconductor charge minus the depletion charge density as indicated below

$$Q_I' = -C_{ox}'\left(V_G - V_{FB} - \phi_s - \gamma\sqrt{\phi_s - \phi_t}\right) \qquad [9]$$

where C'_{ox} is the oxide capacitance per unit area, V_G the gate-to-bulk potential, V_{FB} is the flat-band potential and γ is the body effect factor.

Expanding [9], for constant V_G (3), (4), in power series around an specific value of the surface potential we obtain

$$dQ_I' = nC_{ox}'d\phi_S \qquad [10]$$

where

$$n = 1 + \frac{C_b'}{C_{ox}'} \qquad [11]$$

is the slope factor and C_b' is the depletion capacitance per unit area.

Substituting [10] into [8] and integrating from source to drain, assuming μ constant along the channel, gives the drain current in terms of the inversion charge densities at the source and drain ends of the channel:

$$I_D = \frac{\mu W}{L}\left[\frac{Q_{IS}'^2 - Q_{ID}'^2}{2nC_{ox}'} - \phi_t\left(Q_{IS}' - Q_{ID}'\right)\right] \qquad [12]$$

In some models, *e.g.* (4), (10), *n* is a function of the gate voltage only, while in others, *e.g.* (3), *n* is also a function of the channel voltage.

Consistency of the current equation with the Pao-Sah formulation

To understand the advantage of the choice of *n* as a function of the gate voltage only, let us consider the limit case of [12] in strong inversion (SI).

In SI the inversion charge density is a linear function in terms of the applied voltages (10) as given below

$$Q'_I = -C'_{ox}\left(V_G - V_{T0} - nV_C\right) \qquad [13]$$

where V_{T0} is the equilibrium threshold voltage.

Substituting [13] into [12] and neglecting the linear terms in [12] we obtain the classical SI current law

$$I_D = \mu C'_{ox}\frac{W}{L}\left[V_G - V_{T0} - \frac{n}{2}\left(V_S + V_D\right)\right]\left(V_D - V_S\right). \qquad [14]$$

For n=1 (neglecting the body effect) Eq. [14] reduces to the classical textbook expression (8).

The output conductance of a transistor modeled by [14] is, for a slope factor and mobility independent of the channel voltage, given by

$$g_d = \left.\frac{\partial I_D}{\partial V_D}\right|_{V_G,V_S} = \mu C'_{ox}\frac{W}{L}\left(V_G - V_{T0} - nV_C\right) \qquad [15]$$

complying with Eq. [4].

Let us now consider the all-inversion-regions current equation [12], assuming that *n* and μ are a function of the gate voltage only. The output conductance calculated differentiating [12] is

$$g_d = \left.\frac{\partial I_D}{\partial V_D}\right|_{V_G,V_S} = \frac{\mu W}{L}\left[\frac{-Q'_{ID}}{nC'_{ox}} + \phi_t\right]\frac{dQ'_{ID}}{dV_D}. \qquad [16]$$

From [4] and [16] it follows that

$$dQ'_{ID}\left(\frac{1}{nC'_{ox}} - \frac{\phi_t}{Q'_{ID}}\right) = dV_D. \qquad [17]$$

Equation [17] represents the consistency condition between the Pao-Sah formula [1] and the charge sheet current expression [12]. Using [17] to calculate the derivative of the

channel charge allows simple expressions for all the small signal parameters ((trans)conductances, (trans)capacitances).

The ACM Core Model

Effective mobility and velocity saturation

The effect of carrier velocity saturation is included in the mobility model as (3), (11)

$$\mu = \frac{\mu_s}{1 + \frac{\mu_s}{v_{sat}} \frac{d\phi_s}{dy}} \qquad [18]$$

where v_{sat} is the saturation velocity and μ_s is the mobility of the long-channel device, which is assumed to be a function of V_G only. From [8], [10] and [18] the relation between the differential of channel length and the differential of inversion charge follows

$$dy = -\frac{\mu_s W}{nC'_{ox} I_D} \left(Q'_I - nC'_{ox}\phi_t + \frac{I_D}{W v_{sat}} \right) dQ'_I \qquad [19]$$

Since n depends only on V_G, and I_D is constant along the channel, we can define a virtual charge density that differs from the real charge by a constant term, *i.e.*

$$Q'_V = Q'_I - nC'_{ox}\phi_t + \frac{I_D}{W v_{sat}} . \qquad [20]$$

Using [20], the total inversion charge stored in the channel is easily calculated as (12)

$$Q_I = W(L - \Delta L) \left[\frac{2}{3} \frac{1 + \alpha + \alpha^2}{1 + \alpha} Q'_{VS} + nC'_{ox}\phi_t \right] - \frac{L I_D}{v_{sat}} \qquad [21]$$

where the channel linearity coefficient α is defined as

$$\alpha = \frac{Q'_{VD}}{Q'_{VS}} . \qquad [22]$$

The similarity of this result with the long channel strong inversion model (8) is self-evident, clearly showing the importance of the use of the virtual charge as the key variable. It must be observed that this result is a consequence of the specific choice of the velocity law [18] and the reason behind that choice.

The integration of [19] along the channel allows the calculation of the drain current. Normalizing the charges with respect to the thermal charge $Q'_{IP} = -nC'_{ox}\phi_t$ and the current with respect to the normalization current

$$I_S = \frac{W}{L} \mu_s nC'_{ox} \frac{\phi_t^2}{2} , \qquad [23]$$

the drain current equation is written as

$$i_D = \frac{(q'_{IS} + q'_{ID} + 2)}{1 + \zeta (q'_{IS} - q'_{ID})}(q'_{IS} - q'_{ID}) \qquad [24]$$

where i_D and $q'_{IS(D)}$ are the normalized drain current and source (drain) inversion charges densities, respectively.

The dimensionless short channel parameter ζ is defined as

$$\zeta = \phi_t \mu_s / L v_{sat} \qquad [25]$$

ζ can be regarded as the ratio of the diffusion-related velocity $\mu_s(\phi_t / L)$ at the source of a saturated transistor to the saturation velocity v_{sat}.

The maximum current that can flow in the channel is limited by the maximum carrier velocity. When electrons at the drain end of the channel reach the saturation velocity, the drain current is expressed as

$$i_{Dsat} = \frac{I_{Dsat}}{I_S} = -\frac{W v_{sat} Q'_{IDsat}}{I_S} = \frac{2}{\zeta} q'_{IDsat} \ . \qquad [26]$$

The saturation condition, relating the source charge to the drain charge in saturation is obtained imposing the equality of the general expression of the drain current [24] with the saturated current [25]. Thus, the saturation condition is written as

$$q'_{IS} = \sqrt{1 + \frac{2}{\zeta} q'_{IDsat}} - 1 + q'_{IDsat} \qquad [27]$$

or

$$q'_{IS} = \sqrt{1 + i_{Dsat}} - 1 + \frac{\zeta}{2} i_{Dsat} \, . \qquad [28]$$

The relationship between applied voltages and charges is obtained integrating [17] between source and drain voltages, as

$$\frac{V_{DS}}{\phi_t} = q'_{IS} - q'_{ID} + \ln\left(\frac{q'_{IS}}{q'_{ID}}\right) \, . \qquad [29]$$

The unified charge control model (UCCM)

Integrating [17] between the pinch-off voltage V_P and a generic channel voltage V_C, yields the UCCM. It is interesting to observe that when calculating the charge densities through UCCM we are using exactly the same approximations as in the current formula, guaranteeing a fully consistent model.

To obtain accurate values of the inversion charge the linear approximation of the pinch-off voltage in terms of the gate voltage is not appropriate. Using V_P given by [30], [31], UCCM yields inversion charge values as accurate as those obtained using the surface potential model.

$$V_P = \phi_{sa} - \phi_0 \qquad [30]$$

$$\phi_0 = 2\phi_F + \phi_t\left[1 + ln\left(\frac{n}{n-1}\right)\right] \quad . \qquad [31]$$

ϕ_{sa} is the surface potential calculated disregarding the channel charge and ϕ_F is the Fermi potential in the bulk.

Computer Implementation of the ACM Model

The ACM model was implemented into the ELDO simulator using the UDM (User Definable Model) (13) module. The model code was written in C, since the use of another language implies in a reduction of the performance (speed) of the simulator. The algorithm used for the numerical calculation of the inversion charge in the UCCM is the last one presented in (14). Even it is an iterative algorithm, only one iteration is necessary to obtain relative errors of less than 10^{-7} in the whole inversion range.

For the calculation of the drain current, the factor $1+ \zeta(q'_{IS}-q'_{ID})$ in the denominator of equation [24] is replaced with a continuous and smooth function to avoid discontinuities in the derivatives of the drain current around V_{DS}=0.

Benchmark Tests

The circuit in Figure 2a is employed in the Gummel symmetry test. This test is used to show the symmetry of the forward and reverse modes of operation and the continuity, around the origin, of the drain current and charges as well as their derivatives. As is clear from Figure the ACM model shows the expected behavior but the other two models don't. Even if the derivatives of the current are continuous for HiSIM and PSP, they present a strange behavior around V_{DS}=0.

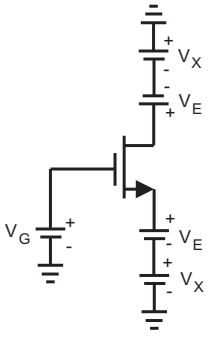

a)

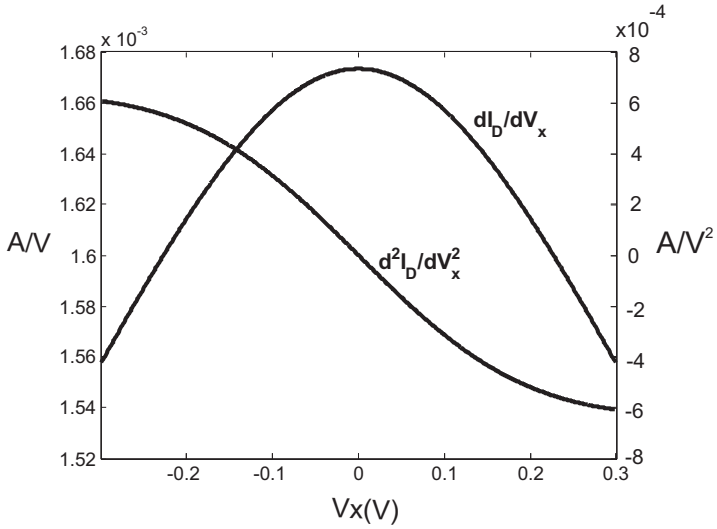

b)

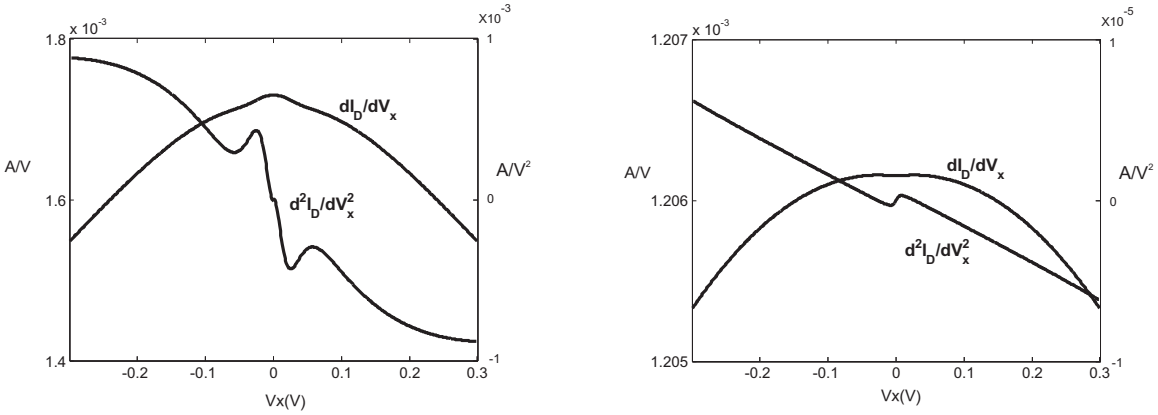

c) d)

Figure 2. Circuit for testing the symmetry of the model at $V_{DS}=0V$ (a). Simulation results for dI_D/dV_X and $d^2I_D/dV^2{}_x$ using the ACM (b), HiSIM (c) and PSP (d) models.

MOSFET current dividers are useful components of analog circuits that can also be used to test the quality of compact models. Figure 3.a shows one such divider. In this array, all transistors have the same dimensions and share a common substrate. A first order analysis of this topology shows that the reference current is successively divided by two. In order to reduce deviations from the expected values owing to short-channel effects, long-channel devices have been employed in the current divider. Fig. 3.b shows that the maximum normalized error using the ACM model does not exceed 0.13% for a 3-decade variation of the reference current I_{REF}. On the other hand the simulations carried out using HiSIM and PSP show high relative error for the current and strange behaviors for the current ratios showing that these models are not able to represent consistently the series association of transistors.

Concerning the code of the models, the ACM use a reduced number of high cost functions compared to the other models as can be shown in Table I. As a consequence the ACM model shows a good speed performance (Table II), that probably can be increased optimizing the C code in ELDO.

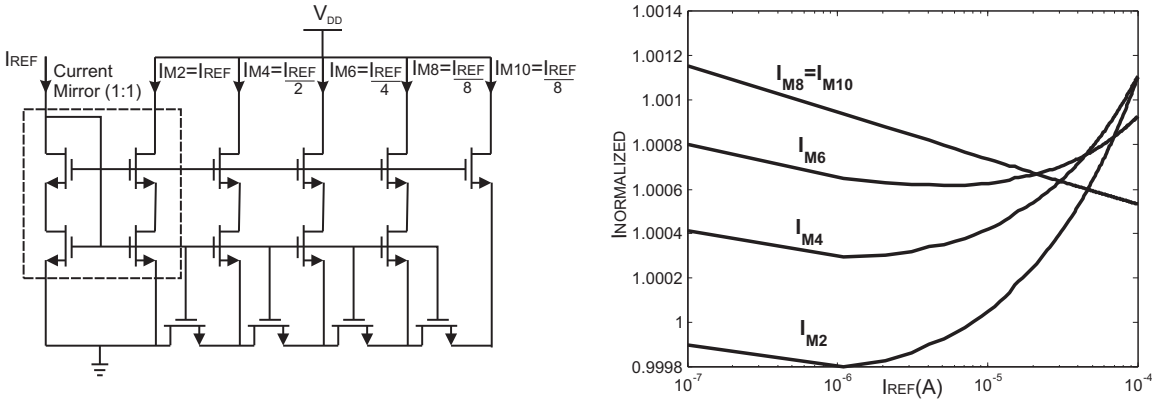

a) b)

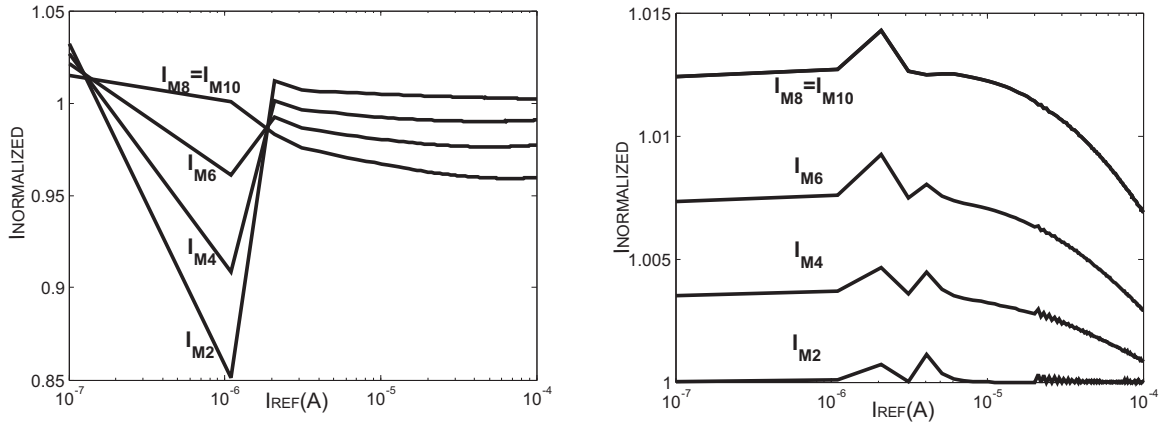

c) d)

Figure 3. MOSFET binary current divider (a). Normalized branch currents vs. input reference current obtained from simulations using the ACM (b) , HiSIM (c) and PSP (d) models in ELDO.

TABLE I. Number of high-cost functions in the main compact models.[1]Data obtained from HiSIM Team (15) and [2]data obtained from PSP team (16).

High-Cost Functions	ACM	HiSIM[1]	PSP[1]	HiSIM[2]	PSP[2]
exp	2	28	123	38	57
log	6	12	68	21	37
pow	3	29	158	28	77
sqrt	11	59	241	68	96
TOTAL	22	138	688	155	267

TABLE II. Normalized simulation times (with respect to ACM_{cap}) using the different models avialbel in ELDO.

Circuit	Analysis	ACM_{cap}	ACM	EKV	MM11	HiSIM	PSP	BSIM4
schmitfast	DC	1s580ms	1.02	0.84	2.14	1.63	1.87	1.16
schmitslow	DC	2s430ms	1.00	0.70	1.75	1.60	1.93	1.28
g1310	TRAN	640ms	0.98	0.92	1.28	1.23	1.31	1.19
hussamp	TRAN	3s020ms	1.07	1.11	1.02	1.06	1.11	1.06
ab_ac	AC	1s400ms	1.03	1.02	2.35	1.63	1.86	1.25
ab_integer	TRAN	1s370ms	1.00	0.98	1.09	1.01	1.13	0.98

Conclusions

The ACM compact model of the MOSFET has been implemented in the electrical simulator ELDO. Benchmarks tests applied to ACM, PSP and HiSIM models have shown better performance of the ACM when compared to the other two models (HISIM and PSP) in several benchmark tests.

Acknowlegments

The authors would like to thank CNPq and CAPES, research agencies of the Brazilian government, for the financial support of this work.

References

1. J. Watts, C. McAndrew, C. Enz, C. Galup-Montoro, G. Gildenblat, C. Hu, R. van Langevelde, M. Miura-Mattausch, R. Rios, C.-T. Sah, “Advanced compact models for MOSFETs,” *Proc. WCM 2005*, pp. 3-12.
2. J. R Brews, “A charge sheet model for the MOSFET,” *Solid-State Electronics*, vol.21, pp.345-355, 1978.
3. M. A. Maher and C. A. Mead, “A physical charge-controlled model for MOS transistors,” in *Advanced Research in VLSI*, P. Losleben (ed.), MIT Press, Cambridge, MA, 1987.
4. A. I. A. Cunha, M. C. Schneider, and C. Galup-Montoro, “An explicit physical model for the long-channel MOS transistor including small-signal parameters,” *Solid-State Electronics*, vol. 38, no 11, pp. 1945-1952, Nov. 1995.
5. G. Gildenblat, X. Li, W. Wu, H. Wang, A. Jha, R. Van Langevelde, G. D. J. Smit, A. J. Scholten, and D. B. M. Klaassen, “PSP: An advanced surface-potential-based MOSFET model for circuit simulation,” *IEEE Trans. Electron Devices*, vol. 53, no. 9, pp. 1979-1993, Sep. 2006.
6. H. C. Pao and C. T. Sah, “Effects of diffusion current on characteristics of metal-oxide (insulator)-semiconductor transistors,” *Solid-State Electron.*, vol. 9, no. 10, pp. 927-937, Oct. 1966.
7. A. I. A. Cunha, M. C. Schneider, and C. Galup-Montoro, “Derivation of the unified charge control model and parameter extraction procedure,” *Solid-State Electronics*, vol. 43, no 3, pp. 481-485, Mar. 1999.
8. C. Galup-Montoro and M. C. Schneider, *MOSFET Modeling for Circuit Analysis and Design*, World Scientific, Singapore, 2007.
9. C. Galup-Montoro, M. C. Schneider, V. C. Pahim and R. Rios, "Comparison of surface-potential-based and charge-based MOSFET core models," *Proc. WCM 2005*, pp. 13 – 18.
10. C. C. Enz, F. Krummenacher, and E. A. Vittoz, “An analytical MOS transistor model valid in all regions of operation and dedicated to low-voltage and low-current applications,” *J. Analog Integr. Circuits Signal Process.*, vol. 8, pp. 83-114, July 1995.
11. O. C. Gouveia Filho, A. I. A. Cunha, M. C. Schneider and C. Galup-Montoro, "Advanced compact model for short-channel MOS transistors," *IEEE Custom Integrated Circuits Conference*, Orlando, FL, USA, pp. 209-212, May 2000.
12. C. Galup-Montoro and M. C. Schneider, "Symbolic charge-based MOSFET model," *Proc. WCM 2006*, pp. 598- 603.
13. *UDM User’s Manual*, Mentor Graphics Corporation, 2005.
14. F. N. Fritsch, R. E. Shafer, and W. P. Crowley, “Solution of the transcendental equation $we^{w}=x$,” *Communications of the ACM*, vol. 16, no.2, pp.123-124, 1973.
15. HiSIM Team, “Important Features of HiSIM and Comparison with PSP”, Nov. 2005. Available online at http://www.eigroup.org/cmc/minutes/default.htm.
16. D.B.M. Klaassen. “Comments on the Perspective of a Commercial SPICE Vendor”, Nov. 2005. Available online at http://www.eigroup.org/cmc/minutes/default.htm.